Journal of Organometallic Chemistry 695 (2010) 2172–2179

Contents lists available at ScienceDirect

Journal of Organometallic Chemistry

journal homepage: www.elsevier.com/locate/jorganchem

The modification of $ArSCH_2(3,5\text{-}Me_2Pz)$ (Ar = phenyl or 2-pyridyl, Pz = pyrazol-1-yl) by organotin group and related reactions

Yun-Fu Xie, Guang-Tong Zeng, Hai-Bin Song, Liang-Fu Tang*

Department of Chemistry, State Key Laboratory of Elemento-Organic Chemistry, Nankai University, Tianjin 300071, People's Republic of China

ARTICLE INFO

Article history:
Received 7 May 2010
Received in revised form
1 June 2010
Accepted 3 June 2010
Available online 15 June 2010

Keywords:
3,5-Dimethylpyrazole
Organotin
Group 6 metal carbonyl complex
S,N chelating ligand
Oxidative addition

ABSTRACT

Reaction of 1-arylthiomethyl-3,5-dimethylpyrazole [$ArSCH_2(3,5\text{-}Me_2Pz)$, Ar = phenyl or 2-pyridyl, Pz = pyrazol-1-yl] with $Mo(CO)_6$ produces complexes $ArSCH_2(3,5\text{-}Me_2Pz)Mo(CO)_4$, while similar reaction with $W(CO)_6$ yields analogous complexes $ArSCH_2(3,5\text{-}Me_2Pz)W(CO)_4$ and concomitant desulfurized complex $(3,5\text{-}Me_2PzH)W(CO)_5$ in the reaction of $PhSCH_2(3,5\text{-}Me_2Pz)$. Succedent treatment of complexes $PhSCH_2(3,5\text{-}Me_2Pz)M(CO)_4$ with $SnCl_4$ gives heterobimetallic complexes $PhSCH_2(3,5\text{-}Me_2Pz)M(CO)_3(Cl)(SnCl_3)$ (M = Mo or W) in good yields. $ArSCH_2(3,5\text{-}Me_2Pz)$ act as S,N chelating bidentate ligands through the sulfur and the pyrazolyl nitrogen atoms in the aforementioned complexes. The modification of $ArSCH_2(3,5\text{-}Me_2Pz)$ by organotin group at the methylene group has been successfully carried out, which yields functionalized ligands $Ph_3SnCH(SAr)(3,5\text{-}Me_2Pz)$. Markedly different reactions are observed, upon treatment of $Ph_3SnCH(SPh)(3,5\text{-}Me_2Pz)$ and $Ph_3SnCH(SPy)(3,5\text{-}Me_2Pz)$ (Py = 2-pyridyl) with $W(CO)_5THF$. The former yields complex $Ph_3SnCH(SPh)(3,5\text{-}Me_2Pz)W(CO)_4$, as well as $PhSCH_2(3,5\text{-}Me_2Pz)W(CO)_4$ with a partial loss of the organotin moiety, while no reaction takes place in the latter. In addition, reaction of $Ph_3SnCH(SPy)(3,5\text{-}Me_2Pz)$ with $Mo(CO)_6$ results in the oxidative addition reaction of the $Sn-C_{sp3}$ bond to the molybdenum(0) atom to yield novel heterometallacyclic complex $CH(SPy)(3,5\text{-}Me_2Pz)Mo(CO)_3SnPh_3$, in which [(2-pyridyl)thiomethyl](3,5-dimethylpyrazol-1-yl)methide acts as a tridentate κ^3-[N,C,N] chelating ligand through the carbon atom, the pyrazolyl and the pyridyl nitrogen atoms, as the sulfur atom does not coordinate to the molybdenum atom anymore. Interestingly, treatment of this heterometallacyclic complex with $P(OR)_3$ (R = Ph or Et) gives rise to the isomerization of the C–S bond to the C–N bond, generating the thione–S coordinated complex $CH(NC_4H_4C=S)(3,5\text{-}Me_2Pz)Mo(CO)_2(P(OR)_3)SnPh_3$, in which the ligand binds in a novel tridentate, monoanionic κ^3-[N,C,S] chelating mode to the molybdenum atom.

1. Introduction

Bis(pyrazol-1-yl)methanes modified by organic functional groups on the bridging carbon atom have drawn extensive attention in recent years, owing to their versatile coordination chemistry towards main group and transition metals [1–3]. Recently, we have developed the modification of bis(pyrazol-1-yl)methanes by organotin groups on the methine carbon atom and proved that the reactivity of these functionalized bis(pyrazol-1-yl)methanes markedly depends on the properties of substituents on the tin atom [4–6]. For example, the reaction of triarylstannylbis(3,5-dimethylpyrazol-1-yl)methane with $W(CO)_5THF$ results in the oxidative addition reaction of the $Sn-C_{sp3}$ bond to the tungsten(0) atom to yield novel four-membered metallacyclic complex $CH(3,5\text{-}Me_2Pz)_2(CO)_3WSnAr_3$ [5], while the analogous reaction of bis(3,5-dimethylpyrazol-1-yl)methane functionalized by organotin halide leads to the oxidative addition of the relatively electrophilic Sn–X (X represents halogen) bond to the tungsten(0) atom [4]. Interestingly, treatments of $CH(3,5\text{-}Me_2Pz)_2(CO)_3WSnAr_3$ with both nucleophilic [7] and electrophilic [8] reagents bring about unusual ring-expansion reactions. These results inspire us to explore the analogous reactivity of other ligands with similar structural features, and 1-phenylthiomethyl-3,5-dimethylpyrazole [9] provides an available case. The lithiation of this ligand at the methylene group has been successfully carried out [9], and the corresponding lithium compound can react with various electrophiles, which makes it as a useful synthetic intermediate. On the other hand, this ligand is anticipated to act as a hybrid S,N chelating ligand. In this paper, we investigate the modification of 1-phenylthiomethyl-3,5-dimethylpyrazole and its analog, namely 1-(2-pyridyl)thiomethyl-3,5-dimethylpyrazole, by organotin group at the methylene group and their related reactions with group 6 metal carbonyl complexes.

* Corresponding author. Fax: +86 22 23502458.
E-mail address: lftang@nankai.edu.cn (L.-F. Tang).

0022-328X/$ – see front matter © 2010 Elsevier B.V. All rights reserved.
doi:10.1016/j.jorganchem.2010.06.006

2. Results and discussion

2.1. Related reaction of 1-phenylthiomethyl-3,5-dimethylpyrazole

1-Phenylthiomethyl-3,5-dimethylpyrazole [$PhSCH_2(3,5\text{-}Me_2Pz)$, Pz = pyrazol-1-yl] has been synthesized for about two decades [9], but its coordination chemistry has drawn little attention. To gain more convictive knowledge on its coordination ability to transition metals and comprehensive foundations for further research, we started our investigations with the reaction of this ligand with $M(CO)_6$ (M = Mo or W) (Scheme 1). Reaction of $PhSCH_2(3,5\text{-}Me_2Pz)$ with $Mo(CO)_6$ produced $PhSCH_2(3,5\text{-}Me_2Pz)Mo(CO)_4$ (**1**), similar reaction with $W(CO)_6$ yielded analogous complex $PhSCH_2(3,5\text{-}Me_2Pz)W(CO)_4$ (**2**) and concomitant desulfurized complex $(3,5\text{-}Me_2PzH)W(CO)_5$. Succedent reaction of complexes $PhSCH_2(3,5\text{-}Me_2Pz)M(CO)_4$ with $SnCl_4$ gave heterobimetallic complexes $PhSCH_2(3,5\text{-}Me_2Pz)M(CO)_3(Cl)(SnCl_3)$ (M = Mo (**3**) and W (**4**), respectively) in good yields.

Complexes **1**–**4** have been characterized by elemental analyses, IR and NMR spectroscopy. These spectroscopic data support the suggested structures. The IR spectra of complexes **1** and **2** show four bands in the carbonyl stretching region, implying a typical *cis*-tetracarbonyl arrangement [10]. While three carbonyl stretching bands are observed in the seven-coordinate complexes **3** and **4**. The structures of complexes **2** and **4** have been further confirmed by X-ray structural analyses.

The crystal structures of complexes **2** and **4** are presented in Figs. 1 and 2, respectively. In these two complexes, 1-phenylthiomethyl-3,5-dimethylpyrazole acts as a hybrid S,N chelating ligand, as expected. The W–N bond distance in complex **2** is 2.264(4) Å, similar to those found in other octahedral tungsten(0) complexes with pyrazol-1-yl ligands, such as 2.292(6) Å in $CH_2(3\text{-}p\text{-}MeOPh\text{-}5\text{-}MeSPz)_2W(CO)_4$ [11] and 2.268(4) Å as well as 2.270(4) Å in $Me_3SiCH(3,5\text{-}Me_2Pz)_2W(CO)_4$ [12]. The W–S bond distance of 2.5398(12) Å is also comparable to those reported in tungsten(0) complexes with thioether ligands, such as 2.543(2) and 2.554(2) Å in $W(CO)_4L$ (L = 1,1,1,1-tetrakis(methylthiomethyl)methane) [13] as well as 2.585(2) and 2.565(2) Å in $(Fc^tBuSMe)W(CO)_4$ (Fc = 1,1′-ferrocenyl) [14]. It is noteworthy that two *cis*-carbonyl groups in this complex considerably deviate from linearity with the W(1)–C(1)–O(1) angle of 171.8(4)° and the W(1)–C(4)–O(4) angle of 172.8(4)°, indicating the presence of steric repulsion between the ligand and these carbonyls. The W–N bond distance of 2.219(4) Å in complex **4** is slightly shorter than that in complex **2**, while the W–S bond distance of 2.5702(15) Å in complex **4** is longer than the corresponding bond distance in complex **2**. These two complexes have similar bite angle N–W–S of 76.23(11)° in complex **4** and 77.18(8)° in complex **2**, respectively.

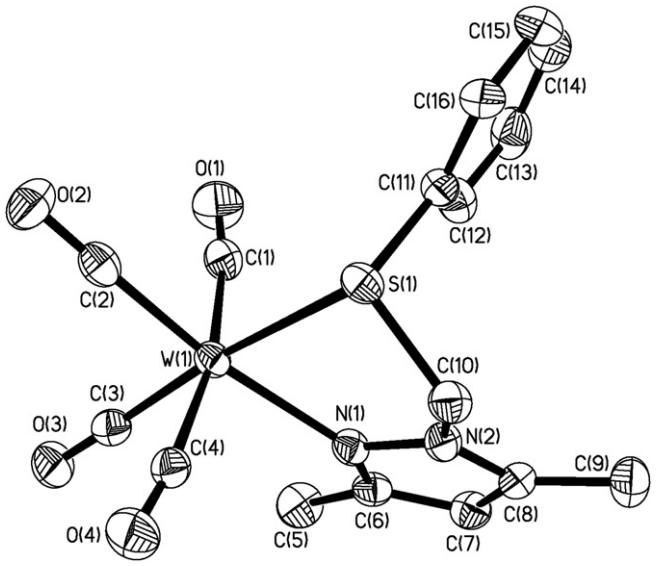

Fig. 1. The molecular structure of **2**. The thermal ellipsoids are drawn at the 30% probability level. Selected bond distances (Å) and angles (°): W(1)–N(1) 2.264(4), W(1)–S(1) 2.5398(12), C(10)–S(1) 1.810(4), C(10)–N(2) 1.438(5) Å; W(1)–C(1)–O(1) 171.8(4), W(1)–C(2)–O(2) 178.5(4), W(1)–C(3)–O(3) 178.1(4), W(1)–C(4)–O(4) 172.8(4), C(1)–W(1)–C(4) 169.80(18), C(3)–W(1)–S(1) 173.61(14), C(3)–W(1)–N(1) 99.22(15), C(10)–S(1)–W(1) 96.46(13), N(1)–W(1)–S(1) 77.18(8), N(2)–C(10)–S(1) 111.3(3)°.

When $PhSCH_2(3,5\text{-}Me_2Pz)$ was treated with butyllithium, the methylene group was deprotonated to afford $LiCH(SPh)(3,5\text{-}Me_2Pz)$ [9]. Treatment of this lithium compound with Ph_3SnCl yielded $Ph_3SnCH(SPh)(3,5\text{-}Me_2Pz)$ (**5**), which was confirmed by X-ray

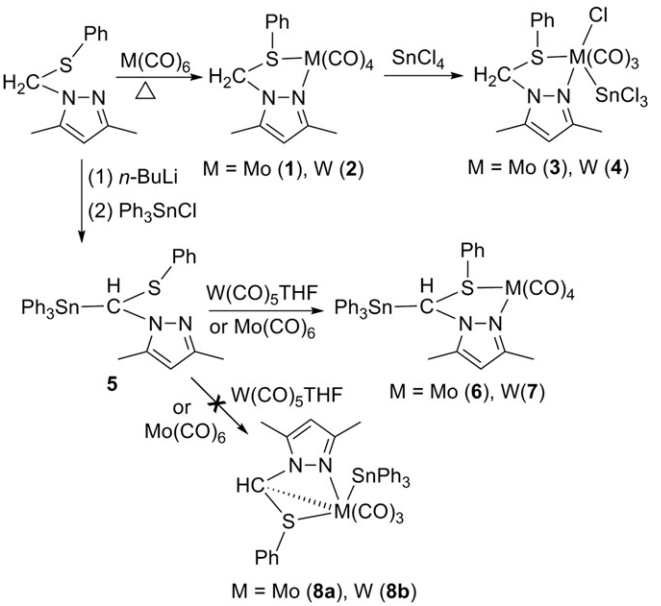

Scheme 1. Related reaction of 1-phenylthiomethyl-3,5-dimethylpyrazole.

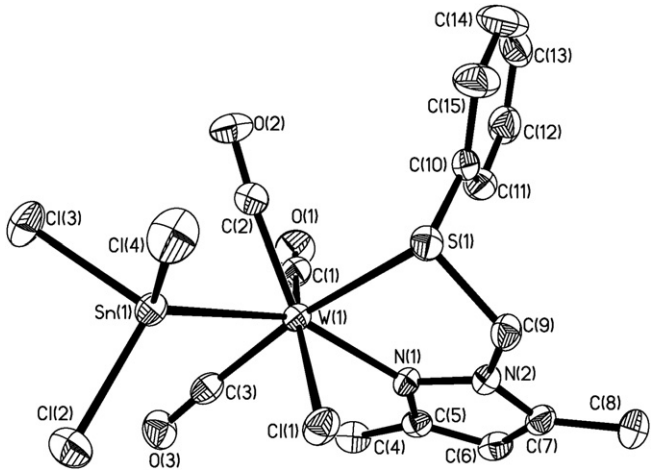

Fig. 2. The molecular structure of **4**. The thermal ellipsoids are drawn at the 30% probability level. Selected bond distances (Å) and angles (°): W(1)–N(1) 2.219(4), W(1)–Cl(1) 2.5409(14), W(1)–S(1) 2.5702(15), W(1)–Sn(1) 2.7711(8), Sn(1)–Cl(4) 2.3483(18), Sn(1)–Cl(2) 2.3487(17), Sn(1)–Cl(3) 2.3897(17), C(9)–S(1) 1.823(6), C(9)–N(2) 1.461(6) Å; C(3)–W(1)–S(1) 170.80(15), N(1)–W(1)–Sn(1) 150.73(10), N(1)–W(1)–S(1) 76.23(11), Cl(2)–Sn(1)–Cl(3) 97.38(7), Cl(3)–Sn(1)–W(1) 120.56(5), C(9)–S(1)–W(1) 98.80(18), N(2)–C(9)–S(1) 111.7(3)°.

diffraction. The molecular structure of ligand **5** is shown in Fig. 3, demonstrating that the tin atom adopts a four-coordinate distorted tetrahedral geometry. The sulfur and pyrazolyl nitrogen atoms do not coordinate to the tin atom, possibly owing to the weak Lewis acidity of the tin atom in tetraalkyltin. Reaction of **5** with $Mo(CO)_6$ or $W(CO)_5THF$ in refluxing THF yielded $Ph_3SnCH(SPh)(3,5\text{-}Me_2Pz)M(CO)_4$ (M = Mo (**6**) and W (**7**), respectively), with certain amount of complex **2** in the case of tungsten. No oxidative addition product of the Sn–C_{sp3} or Sn–C_{sp2} bond to the molybdenum(0) or tungsten (0) atom was obtained.

Complexes **6** and **7** are air-stable in the solid state, but their solutions, especially the solution of complex **6**, are air-sensitive. These two complexes have been characterized by spectroscopic methods. The carbonyl stretches in their IR spectra match the pattern for a typical *cis*-tetracarbonyl arrangement around the metal atom, similar to those in complexes **1** and **2**. The proton signals assigned for pyrazole ring are considerably shifted to lower field, compared with those in ligand **5**. Four ^{13}C NMR signals of the carbonyls have been observed in these two complexes, implying that four carbonyls are inequivalent possibly owing to these substituents in the ligand preventing their free rotation in solution. The molecular structure of complex **7** is shown in Fig. 4. To reduce the steric repulsion between each other, the phenyl group is *trans* to the triphenyltin moiety. Four carbonyls in the complex deviate from linearity because of steric repulsion between the ligand and these carbonyls. The W–N and W–S bond distances are 2.237(3) and 2.5236(9) Å, respectively, similar to the corresponding bond distances in complex **2**. Some angles around the Sn(1) atom (such as the angles C(16)–Sn(1)–C(23) of 119.36(13)° and C(16)–Sn(1)–C(29) of 94.78(12)°) markedly deviate from the tetrahedral geometry of the sp^3 hybridized tin atom. The deviation is more remarkable than that in the free ligand **5** (such as the angles C(7)–Sn(1)–C(19) of 117.63(13)° and C(13)–Sn(1)–C(19) of 100.82(12)° in **5**) since the chelating coordination to the tungsten atom increases the steric congestion around the tin atom in complex **7**.

Although no oxidative addition reaction takes place during the reaction of ligand **5** with $Mo(CO)_6$ or $W(CO)_5THF$, the isolation of

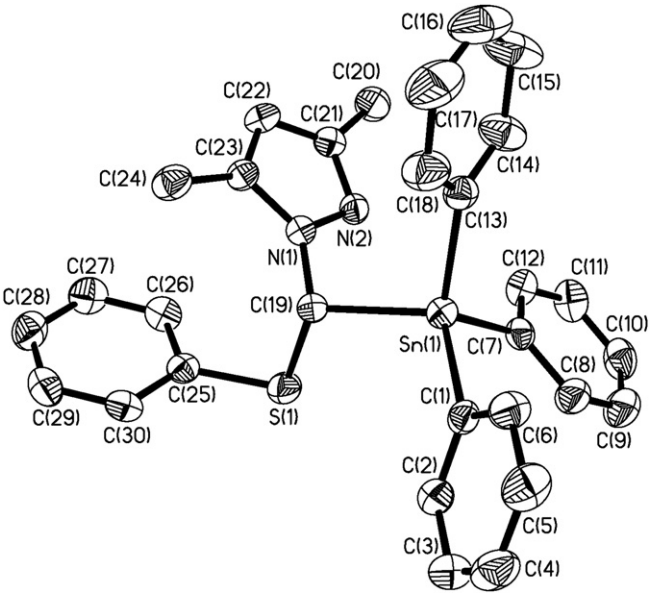

Fig. 3. The molecular structure of **5**. The thermal ellipsoids are drawn at the 30% probability level. Selected bond distances (Å) and angles (°): Sn(1)–C(7) 2.132(4), Sn(1)–C(19) 2.191(3), C(19)–S(1) 1.811(3), C(25)–S(1) 1.785(3), C(19)–N(1) 1.451(4) Å; C(7)–Sn(1)–C(19) 117.63(13), C(13)–Sn(1)–C(19) 100.82(12), C(19)–S(1)–C(25) 100.61(14), N(1)–C(19)–S(1) 113.4(2), S(1)–C(19)–Sn(1) 112.60(15)°.

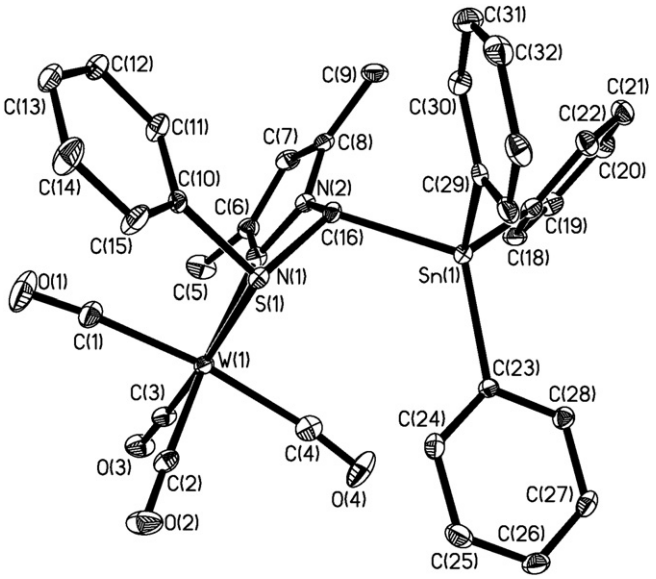

Fig. 4. The molecular structure of **7**. The thermal ellipsoids are drawn at the 30% probability level. Selected bond distances (Å) and angles (°): W(1)–N(1) 2.237(3), W(1)–S(1) 2.5236(9), Sn(1)–C(16) 2.216(3), Sn(1)–C(29) 2.126(4), C(16)–N(2) 1.455(4), C(16)–S(1) 1.805(3) Å; W(1)–C(1)–O(1) 174.7(4), W(1)–C(2)–O(2) 177.6(4), W(1)–C(3)–O(3) 178.2(4), W(1)–C(4)–O(4) 172.8(4), C(3)–W(1)–S(1) 174.97(11), N(1)–W(1)–S(1) 76.87(8), N(2)–C(16)–S(1) 112.3(2), N(2)–C(16)–Sn(1) 122.6(2), C(16)–Sn(1)–C(23) 119.36(13), C(16)–Sn(1)–C(29) 94.78(12), C(10)–S(1)–C(16) 103.88(16), C(10)–S(1)–W(1) 112.24(11), C(16)–S(1)–W(1) 100.55(12)°.

complex **2** in the case of tungsten suggests that the Sn–C_{sp3} bond is still active. The oxidative addition products **8** are not obtained may be as a result of their poor stability, led by the ring strain of the small three-membered metallacycle. We suppose that similar oxidative addition reaction can arise, if this small metallacycle is enlarged through other coordination atoms introduced by substituting the heteroaryl groups for the phenyl group, such as the replacement of the phenyl group by 2-pyridyl. Thus 1-(2-pyridyl)thiomethyl-3,5-dimethylpyrazole [$PySCH_2(3,5\text{-}Me_2Pz)$] (**9**) was designed and synthesized.

2.2. Synthesis and related reaction of 1-(2-pyridyl)thiomethyl-3,5-dimethylpyrazole

Ligand **9** was readily obtained by the reaction of 2-mercaptopyridine with 1-chloromethyl-3,5-dimethylpyrazole under basic conditions, which is expected to act as a potential multidentate ligand. Reaction of this ligand with $Mo(CO)_6$ or $W(CO)_5THF$ in refluxing THF yielded complexes $PySCH_2(3,5\text{-}Me_2Pz)M(CO)_4$ (M = Mo (**10**) and W (**11**), respectively) (Scheme 2). Their IR spectra exhibit four bands for the carbonyl stretching, similar to those in complexes **1** and **2** as well as **6** and **7**. The ^1H NMR spectra of these two complexes also exhibit the expected signals of the ligand and peak multiplicities for the pyridyl group. It is worthy of pointing out that the protons of the methylene group of complex **11** display an AB resonance at room temperature, which is also observed in complex **2**. These may be the results of the inversion of the conformation of the five-membered metallacycle as well as the free rotation of the phenyl or pyridyl group being slowed down due to the steric repulsion among substituents. At the same time, four carbonyl signals are observed in the ^{13}C NMR spectra of complexes **10** and **11**, like those in complexes **6** and **7**.

The coordination mode of ligand **9** in complexes **10** and **11** was established by the X-ray crystal diffraction analyses of complex **10**. As shown in Fig. 5, $PySCH_2(3,5\text{-}Me_2Pz)$ acts as a S,N chelating bidentate ligand through the sulfur and pyrazolyl nitrogen atoms,

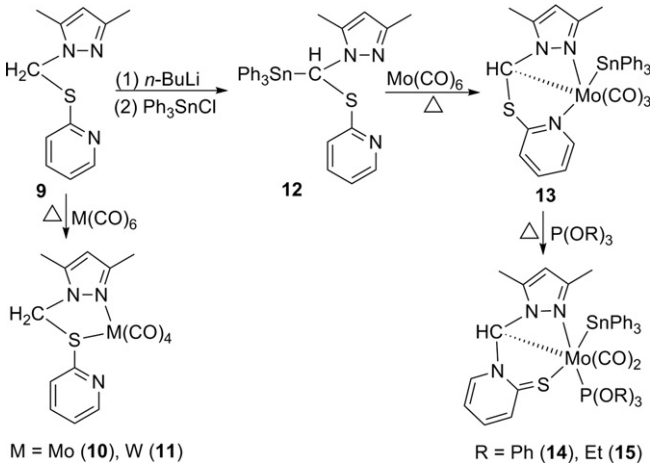

Scheme 2. Related reaction of 1-(2-pyridyl)thiomethyl-3,5-dimethylpyrazole.

and the pyridyl nitrogen atom does not coordinate to the molybdenum atom. The fundamental molecular framework is similar to that in complex **2**. For example, two distorted *cis*-carbonyls are observed in these two complexes. Their structural parameters are also very analogous since the covalent radii of molybdenum is close to that of tungsten [15], such as similar M–N and M–S bond distances as well as similar bite angle of N–M–S.

The modification of ligand **9** by organotin group at the methylene group has been successfully carried out, as described above for $PhSCH_2(3,5\text{-}Me_2Pz)$. Ligand **9** could be smoothly lithiated at the methylene group and subsequently reacted with Ph_3SnCl to yield $Ph_3SnCH(SPy)(3,5\text{-}Me_2Pz)$ (**12**). The reactivity of ligand **12** is significantly different from that of ligand **5**. The reaction of ligand **12** with $Mo(CO)_6$ resulted in the oxidative addition reaction of the $Sn–C_{sp3}$ bond to the molybdenum(0) atom to yield novel heterometallacyclic complex $CH(SPy)(3,5\text{-}Me_2Pz)Mo(CO)_3SnPh_3$ (**13**). However, upon heating ligand **12** with $W(CO)_5THF$ in refluxing THF, no reaction took place. When this reaction was carried out at elevated temperature, the ligand decomposed and no isolable complex was obtained.

Complex **13** is air-stable in the solid state, and its solution can be manipulated in the air without notable decomposition. The proton signal of the CH group (4.18 ppm) in the complex is markedly shifted to higher field, compared with that in free ligand **12** (5.97 ppm), possibly owing to the relatively smaller electronegativity of molybdenum than that of tin [16]. The structure of complex **13** has been confirmed by X-ray crystallography. As seen in Fig. 6, the pyridyl nitrogen atom instead of the sulfur atom coordinates to the molybdenum atom as mentioned previously, resulting in the formation of novel four- and five-membered heterometallacycles. [(2-Pyridyl)thiomethyl](3,5-dimethylpyrazol-1-yl)methide acts as a tridentate κ^3-[N,C,N] chelating ligand through the carbon atom as well as the pyrazolyl and the pyridyl nitrogen atoms. The Mo–$N_{pyridyl}$ bond distance of 2.258(5) Å is slightly longer than the Mo–$N_{pyrazolyl}$ bond distance of 2.208(5) Å, but similar to that in complex **10** (2.263(2) Å). The structural parameters related to the four-membered metallacycle are comparable to those in other four-membered heterometallacyclic complexes with similar structural features, such as $CH(3,5\text{-}^iPr_2Pz)_2W(CO)_3SnPh_3$ [5] and $CH(3,5\text{-}Me_2Pz)_2W(CO)_3Cl$ [17]. For example, the angle N–C–M in these complexes is very close to 90°. In addition, the four-membered heterometallacycle is nearly planar, with a mean deviation from the plane of 0.0316 Å.

Complex **13** is expected to have unusual reactivity, like $CH(3,5\text{-}Me_2Pz)_2W(CO)_3SnPh_3$ [7,8], owing to the polar metal–carbon bond and ring strain in the four-membered metallacycle. Herein, we find that the reaction of this complex with $P(OR)_3$ is remarkably different from the corresponding reaction of $CH(3,5\text{-}Me_2Pz)_2W(CO)_3SnPh_3$ with $P(OR)_3$ [7]. Treatment of complex **13** with $P(OR)_3$ (R = Ph or Et) results in the formation of complexes **14** and **15**, in which the four-membered metallacycle is not broken down. The crystal structural analyses of complex **14** show that complex **13** undergoes Mo–$N_{pyridyl}$ bond cleavage, and subsequently isomerizes to give the thione–S coordinated complex (Fig. 7). The ligand binds in a novel tridentate, monoanionic κ^3-[N,C,S] chelating mode to the molybdenum atom in this complex.

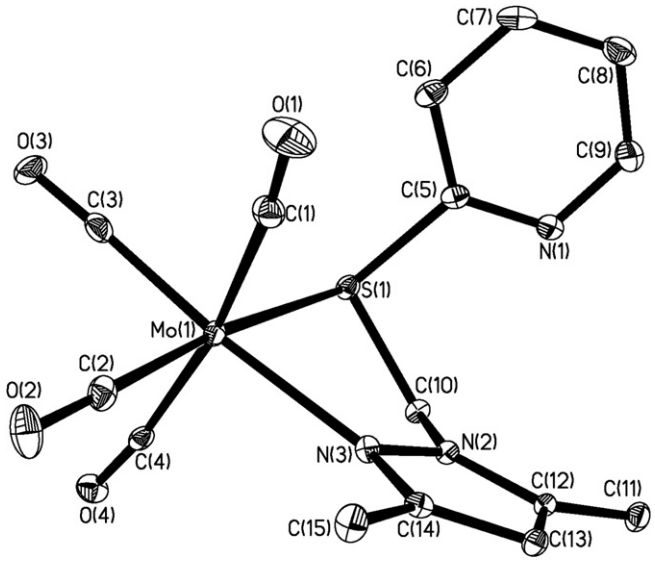

Fig. 5. The molecular structure of **10**. The thermal ellipsoids are drawn at the 30% probability level. Selected bond distances (Å) and angles (°): Mo(1)–N(3) 2.263(2), Mo(1)–S(1) 2.5582(9), C(10)–N(2) 1.453(3), C(10)–S(1) 1.805(2) Å; Mo(1)–C(1)–O(1) 172.8(2), Mo(1)–C(2)–O(2) 178.9(2), Mo(1)–C(3)–O(3) 178.1(2), Mo(1)–C(4)–O(4) 172.3(2), C(2)–Mo(1)–S(1) 173.40(7), C(2)–Mo(1)–N(3) 98.31(9), N(3)–Mo(1)–S(1) 76.87(6), N(2)–C(10)–S(1) 111.02(15), C(5)–S(1)–C(10) 100.33(11), C(10)–S(1)–Mo(1) 96.19(8)°.

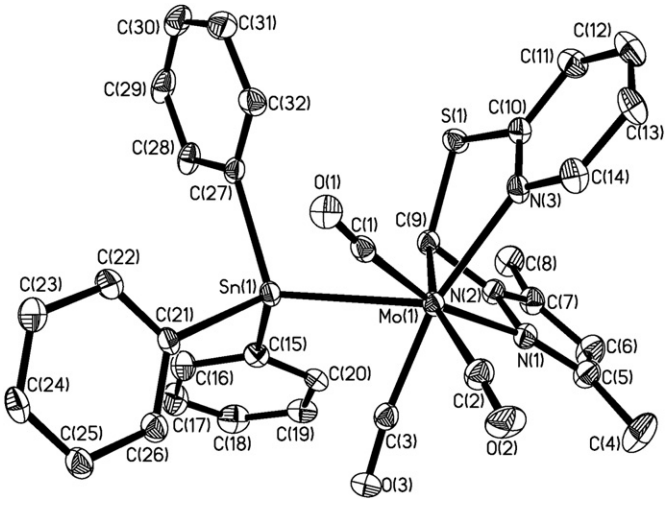

Fig. 6. The molecular structure of **13**. The thermal ellipsoids are drawn at the 30% probability level. The uncoordinated solvent molecules have been omitted for clarity. Selected bond distances (Å) and angles (°): Mo(1)–C(9) 2.310(6), Mo(1)–Sn(1) 2.7690(15), Mo(1)–N(1) 2.208(5), Mo(1)–N(3) 2.258(5), C(9)–S(1) 1.799(6), C(10)–S(1) 1.735(6), C(9)–N(2) 1.471(8) Å; N(1)–Mo(1)–N(3) 82.37(19), N(1)–Mo(1)–C(9) 61.92(19), C(3)–Mo(1)–N(3) 166.4(2), C(3)–Mo(1)–N(1) 87.5(2), C(21)–Sn(1)–C(27) 103.2(2), C(21)–Sn(1)–Mo(1) 117.74(15), C(9)–S(1)–C(10) 99.9(3), N(2)–C(9)–S(1) 110.3(4), N(2)–C(9)–Mo(1) 90.2(3), S(1)–C(9)–Mo(1) 115.0(3), N(1)–N(2)–C(9) 110.1(5)°.

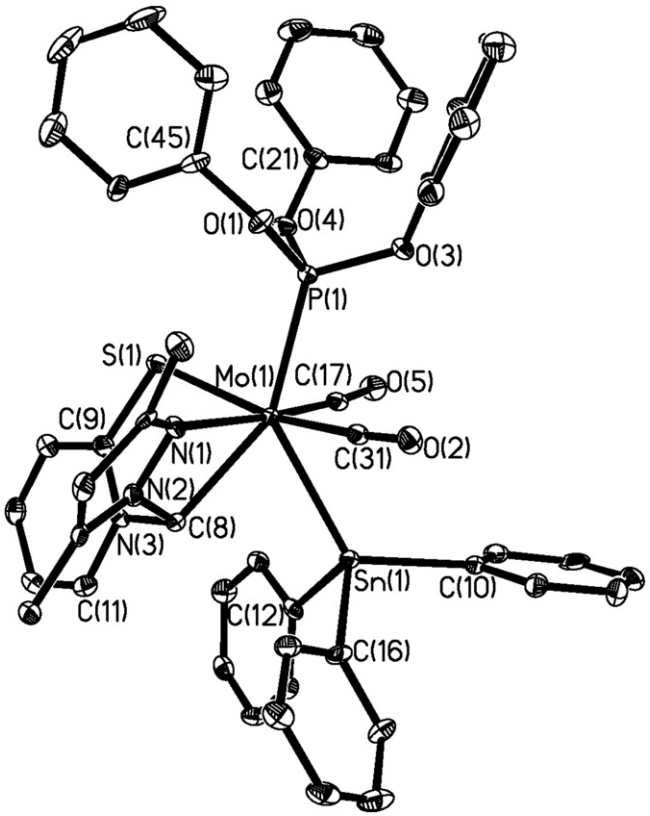

Fig. 7. The molecular structure of **14**. The thermal ellipsoids are drawn at the 30% probability level. Selected bond distances (Å) and angles (°): Mo(1)–Sn(1) 2.7432(10), Mo(1)–N(1) 2.239(6), Mo(1)–C(8) 2.312(7), Mo(1)–P(1) 2.3891(19), Mo(1)–S(1) 2.5229(19), P(1)–O(1) 1.606(5), C(8)–N(3) 1.484(9), C(8)–N(2) 1.447(8), C(9)–S(1) 1.713(7) Å; C(10)–Sn(1)–C(16) 102.1(3), C(10)–Sn(1)–Mo(1) 123.35(17), C(31)–Mo(1)–S(1) 164.6(2), O(1)–P(1)–O(3) 99.1(3), C(9)–S(1)–Mo(1) 104.6(3), N(2)–C(8)–N(3) 109.4(5), P(1)–Mo(1)–Sn(1) 137.09(5)°.

The notable change of the coordination mode is evidently reflected by the NMR spectra of complexes **14** and **15**. The proton signal of the CH group in these two complexes (5.28 ppm in complex **14** and 5.30 ppm in complex **15**, respectively) is shifted to lower field in comparison to the signal in complex **13**. Moreover, the shift of the ^{13}C NMR signal of the CH group is more noticeable, from 49.1 ppm in complex **13** to 83.1 ppm in complex **14** and 83.3 ppm in complex **15**, respectively. Other marked changes are the chemical shifts of the protons and carbons involving the pyridyl group. A large upfield shift for the proton, related to the pyridyl group in complex **13**, is observed in complexes **14** (6.19 ppm) and **15** (6.28 ppm). At the same time, a carbon appears farther downfield (177.8 ppm) in the ^{13}C NMR spectra of complexes **14** and **15**, and this signal is split into a doublet by the phosphorus atom.

2.3. Possible pathway of the formation of complexes *14* and *15*

The isomerization of the C–S bond to the C–N bond has been observed in bis [18] and tri(thioimidazolyl)methanes [19], and an intramolecular 1,3-sigmatropic rearrangement mechanism for this isomerization has been proposed [18]. Based on this proposal and other known facts, a plausible pathway of the formation of complexes **14** and **15** is depicted in Scheme 3. Initially, the phosphorus ligand replaces the pyridyl group, leading to the cleavage of the Mo–$N_{pyridyl}$ bond to afford a free pyridyl group. Subsequently, an intramolecular 1,3-sigmatropic rearrangement gives rise to the isomerization of the C–S bond to the C–N bond to generate the thione intermediate. Finally, the sulfur atom substitutes a carbonyl group to give complex

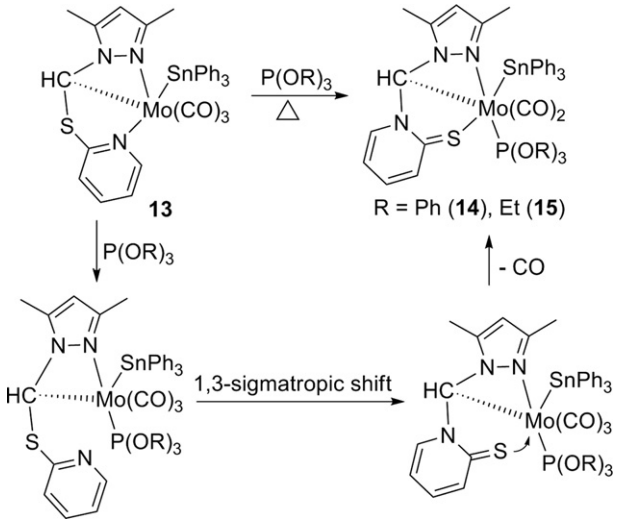

Scheme 3. Possible pathway of the formation of complexes **14** and **15**.

14 or **15**. The preference of the relatively soft molybdenum atom for the soft sulfur atom instead of the hard nitrogen atom is possibly one of the potential reasons of the isomerization.

In conclusion, the modification of 1-arylthiomethyl-3,5-dimethylpyrazole [$ArSCH_2(3,5\text{-}Me_2Pz)$] by organotin group at the methylene group and their related reactions with $M(CO)_6$ have been carried out. $ArSCH_2(3,5\text{-}Me_2Pz)$ act as S,N chelating bidentate ligands through the sulfur and pyrazolyl nitrogen atoms in their complexes. The reactivity of these functionalized ligands $Ph_3SnCH(SAr)(3,5\text{-}Me_2Pz)$ is different from that of $Ph_3SnCH(3,5\text{-}Me_2Pz)_2$. Upon treatment of the former with $W(CO)_5THF$, no analogous oxidative addition reaction of the Sn–C_{sp3} bond to the tungsten(0) atom, as described in the similar reaction of the latter with $W(CO)_5THF$ [5], is observed. However, heating $Ph_3SnCH(SPy)(3,5\text{-}Me_2Pz)$ and $Mo(CO)_6$ leads to the oxidative addition reaction of the Sn–C_{sp3} bond to the molybdenum(0) atom, yielding a novel heterometallacyclic complex $CH(SPy)(3,5\text{-}Me_2Pz)Mo(CO)_3SnPh_3$, in which the sulfur atom does not coordinate to the molybdenum atom anymore. Although some similar structural features are observed in $CH(SPy)(3,5\text{-}Me_2Pz)Mo(CO)_3SnPh_3$ and $CH(3,5\text{-}Me_2Pz)_2W(CO)_3SnPh_3$, they exhibit different reactivity. Reaction of the former with $P(OR)_3$ gives rise to the isomerization of the C–S bond to the C–N bond to generate the thione–S coordinated complex, instead of the P–O exchange reaction like that in the latter [7].

3. Experimental

Solvents were dried by standard methods and distilled prior to use. All reactions were carried out under an argon atmosphere. NMR spectra were recorded on a Bruker 400 spectrometer using $CDCl_3$ as solvent unless otherwise noted, and the chemical shifts were reported in ppm with respect to reference standards (internal $SiMe_4$ for ^1H NMR and ^{13}C NMR spectra, external 85% H_3PO_4 aqueous solution for ^{31}P NMR spectra). IR spectra were obtained from a Nicolet 380 spectrometer as KBr discs. Elemental analyses were carried out on an Elementar Vairo EL analyzer. 1-Phenylthiomethyl-3,5-dimethylpyrazole [$PhSCH_2(3,5\text{-}Me_2Pz)$] [9] was prepared by the published method.

3.1. Synthesis of $PhSCH_2(3,5\text{-}Me_2Pz)Mo(CO)_4$ (*1*)

The solution of $Mo(CO)_6$ (0.24 g, 0.91 mmol) and $PhSCH_2(3,5\text{-}Me_2Pz)$ (0.20 g, 0.91 mmol) in THF (20 ml) was stirred and heated at

reflux for 6 h. After cooling to room temperature, the solvent was removed *in vacuo*, and the residue was purified by column chromatography on silica using ethyl acetate/hexane (*V*:*V* = 1:10) as eluent. The green-yellow eluate was concentrated to dryness under a reduced pressure, and the residue was recrystallized from CH_2Cl_2/hexane to give green-yellow crystals of **1**. Yield: 0.24 g (62%). ^{1}H NMR: δ 2.10, 2.50 (s, s, 3H, 3H, CH_3), 5.03 (s, br, 2H, CH_2), 5.99 (s, 1H, H^4 of pyrazole), 7.09–7.12, 7.29–7.39 (m, m, 2H, 3H, C_6H_5) ppm. ^{13}C NMR: δ 12.3, 16.5 (*C*H$_3$), 58.4 (*C*H$_2$), 108.0 (C^4 of pyrazole), 129.9, 130.8, 131.2, 132.8 (C_6H_5), 142.1, 153.8 (C^3 and C^5 of pyrazole), 219.6, 220.3 (*C*O) ppm. IR: ν_{CO} = 2020.4 (s), 1897.2 (sh), 1875.2 (vs), 1823.7 (vs) cm^{-1}. Anal. Calc. for $C_{16}H_{14}MoN_2O_4S$: C, 45.08; H, 3.31; N, 6.57. Found: C, 44.78; H, 3.68; N, 6.55%.

3.2. Synthesis of PhSCH$_2$(3,5-Me$_2$Pz)W(CO)$_4$ (**2**)

The solution of W(CO)$_6$ (0.32 g, 0.91 mmol) and PhSCH$_2$(3,5-Me$_2$Pz) (0.20 g, 0.91 mmol) in dioxane (40 ml) was stirred and heated at reflux for 5 h. After cooling to room temperature, the solvent was removed *in vacuo*, and the residue was purified by column chromatography on silica using ethyl acetate/CH_2Cl_2/hexane (*V*:*V*:*V* = 2:5:20) as eluent to yield two products. The first green-yellow band was confirmed as known complex (3,5-Me$_2$PzH)W(CO)$_5$ (29 mg, 7.6%) according to its spectroscopic data. ^{1}H NMR: δ 2.31 (s, 6H, CH_3), 5.93 (s, 1H, H^4 of pyrazole), 9.35 (s, br, 1H, N*H*) ppm. IR: ν_{NH} = 3386.2 (m), ν_{CO} = 2074.7 (w), 1947.0 (s), 1919.1 (vs), 1832.5 (vs) cm^{-1}. The second green-yellow band was confirmed as compound **2** (0.11 g, 24%). ^{1}H NMR: δ 2.16, 2.53 (s, s, 3H, 3H, CH_3), 5.02, 5.18 (d, *J* = 11.4 Hz, d, *J* = 11.4 Hz, 1H, 1H, CH_2), 6.02 (s, 1H, H^4 of pyrazole), 7.08–7.10, 7.31–7.42 (m, m, 2H, 3H, C_6H_5) ppm. ^{13}C NMR: δ 12.4, 17.2 (*C*H$_3$), 58.4 (*C*H$_2$), 107.8 (C^4 of pyrazole), 129.8, 130.8, 131.3, 132.7 (C_6H_5), 141.7, 154.1 (C^3 and C^5 of pyrazole), 210.2, 210.8 (*C*O) ppm. IR: ν_{CO} = 2013.9 (s), 1890.4 (sh), 1867.9 (vs), 1817.8 (vs) cm^{-1}. Anal. Calc. for $C_{16}H_{14}N_2O_4SW$: C, 37.37; H, 2.74; N, 5.45. Found: C, 37.39; H, 2.75; N, 5.54%.

3.3. Reaction of **1** and **2** with SnCl$_4$

SnCl$_4$ (0.4 mmol) was added by syringe to a stirred solution of **1** or **2** (0.4 mmol) in 20 ml of CH_2Cl_2. After continuously stirring at room temperature for 2 h, the solution was concentrated to dryness under a reduced pressure, and the residue was recrystallized from CH_2Cl_2/hexane to give orange-red crystals of **3** or **4**.

3.3.1. PhSCH$_2$(3,5-Me$_2$Pz)Mo(CO)$_3$(Cl)SnCl$_3$ (**3**)

This compound was obtained by the reaction of **1** with SnCl$_4$. Yield: 91%. ^{1}H NMR (DMSO-d_6): δ 1.97, 2.07 (s, s, 3H, 3H, CH_3), 5.48 (s, 2H, CH_2), 5.81 (s, 1H, H^4 of pyrazole), 7.31–7.35, 7.40–7.43 (m, m, 3H, 2H, C_6H_5) ppm. IR: ν_{CO} = 2026.2 (vs), 1962.5 (vs), 1933.3 (vs) cm^{-1}. Anal. Calc. for $C_{15}H_{14}Cl_4MoN_2O_3SSn$: C, 27.35; H, 2.14; N, 4.25. Found: C, 27.11; H, 2.15; N, 4.29%.

3.3.2. PhSCH$_2$(3,5-Me$_2$Pz)W(CO)$_3$(Cl)SnCl$_3$ (**4**)

This compound was obtained by the reaction of **2** with SnCl$_4$. Yield: 90%. ^{1}H NMR (DMSO-d_6): δ 1.97, 2.07 (s, s, 3H, 3H, CH_3), 5.47 (s, 2H, CH_2), 5.81 (s, 1H, H^4 of pyrazole), 7.30–7.36, 7.40–7.43 (m, m, 3H, 2H, C_6H_5) ppm. IR: ν_{CO} = 2019.0 (s), 1945.6 (s), 1923.9 (vs) cm^{-1}. Anal. Calc. for $C_{15}H_{14}Cl_4N_2O_3SSnW$: C, 24.13; H, 1.89; N, 3.75. Found: C, 23.66; H, 2.32; N, 3.41%.

3.4. Synthesis of Ph$_3$SnCH(SPh)(3,5-Me$_2$Pz) (**5**)

A hexane solution of *n*-BuLi (2.5 M, 4.0 ml, 10 mmol) was added to a solution of PhSCH$_2$(3,5-Me$_2$Pz) (2.18 g, 10 mmol) in THF (75 ml) at −70 °C, and the mixture was stirred for 1 h at that temperature. To the mixture was added a solution of Ph$_3$SnCl (3.86 g, 10 mmol) in THF (25 ml). The reaction mixture was stirred at −70 °C for 1 h, allowed to reach room temperature slowly and stirred for additional 1 h. The solvent was removed *in vacuo*, and the residue was recrystallized from hexane to give white crystals of **5**. Yield: 4.54 g (80%). ^{1}H NMR: δ 1.69, 2.21 (s, s, 3H, 3H, CH_3), 5.70 (s, br, 2H, C*H* and H^4 of pyrazole), 7.30–7.41, 7.69–7.72 (m, m, 14H, 6H, SnC_6H_5 and SC_6H_5) ppm. ^{13}C NMR: δ 11.0, 13.4 (*C*H$_3$), 58.0 (*C*H), 106.3 (C^4 of pyrazole), 128.4, 128.6, 128.9, 129.4, 129.5, 136.6, 137.4, 139.0, 139.5, 147.3 (SnC_6H_5, SC_6H_5 as well as C^3 and C^5 of pyrazole) ppm. Anal. Calc. for $C_{30}H_{28}N_2SSn$: C, 63.51; H, 4.97; N, 4.94. Found: C, 63.50; H, 5.33; N, 5.10%.

3.5. Reaction of **5** with Mo(CO)$_6$

The solution of Mo(CO)$_6$ (0.16 g, 0.60 mmol) and **5** (0.34 g, 0.60 mmol) dissolved in THF (40 ml) was heated at reflux for 5 h. After cooling to room temperature, the solvent was removed under reduced pressure, and the residue was purified by column chromatography on silica using CH_2Cl_2/hexane (*V*:*V* = 1:1) as eluent. The green-yellow eluate was concentrated to dryness under reduced pressure to give a green-yellow solid of Ph$_3$SnCH(SPh)(3,5-Me$_2$Pz)Mo(CO)$_4$ (**6**). Yield: 0.26 g (56%). ^{1}H NMR: δ 1.82,2.33(s, s, 3H, 3H, CH_3), 5.67 (s, 1H, C*H*), 5.81 (s, 1H, H^4 of pyrazole), 6.98–7.01, 7.18–7.19, 7.26–7.33 (m, m, m, 2H, 3H, 15H, SnC_6H_5 and SC_6H_5). ^{13}C NMR: δ 12.6, 16.8 (*C*H$_3$), 59.2 (*C*H), 108.2 (C^4 of pyrazole), 127.6, 129.1, 129.4, 129.7, 130.2, 135.9, 137.0, 140.0, 141.2, 153.0 (SnC_6H_5, SC_6H_5 as well as C^3 and C^5 of pyrazole), 204.9, 206.5, 219.5, 220.1 (*C*O). IR: ν_{CO} = 2018.0 (s), 1905.3 (vs), 1880.7 (vs), 1842.9 (vs) cm^{-1}. Anal. Calc. for $C_{34}H_{28}MoN_2O_4SSn$: C, 52.67; H, 3.64; N, 3.61. Found: C, 52.71; H, 3.84; N, 3.69%.

3.6. Reaction of **5** with W(CO)$_5$THF

Compound **5** (0.17 g, 0.30 mmol) was added to a solution of W(CO)$_5$THF in THF, prepared *in situ* by the irradiation of a solution of W(CO)$_6$ (0.11 g, 0.3 mmol) in THF (40 ml) for 8 h, and the mixture was stirred and heated at reflux for 4 h. The solvent was removed *in vacuo*, and the residue was purified by column chromatography on silica using ethyl acetate/hexane (*V*:*V* = 1:4) as eluent to yield two products. The first green-yellow band was confirmed as Ph$_3$SnCH(SPh)(3,5-Me$_2$Pz)W(CO)$_4$ (**7**) (28 mg, 11%). ^{1}H NMR: δ 1.94, 2.45 (s, s, 3H, 3H, CH_3), 5.80 (s, $^2J_{Sn-H}$ = 17.8 Hz, 1H, C*H*), 5.91 (s, 1H, H^4 of pyrazole), 7.04–7.08, 7.28–7.32, 7.36–7.41 (m, m, m, 2H, 4H, 14H, SnC_6H_5 and SC_6H_5) ppm. ^{13}C NMR: δ 13.0, 17.8 (*C*H$_3$), 60.6 (*C*H), 108.2 (C^4 of pyrazole), 127.8, 129.7, 129.8, 130.1, 130.2, 135.8, 137.0, 139.9, 141.1, 153.6 (SnC_6H_5, SC_6H_5 as well as C^3 and C^5 of pyrazole), 202.1, 203.0, 210.3, 210.6 (*C*O) ppm. IR: ν_{CO} = 2017.1 (s), 1902.9 (vs), 1875.5 (vs), 1824.6 (vs) cm^{-1}. Anal. Calc. for $C_{34}H_{28}N_2O_4SSnW$: C, 47.31; H, 3.27; N, 3.25. Found: C, 47.05; H, 3.60; N, 3.24%. The second green-yellow band was confirmed as compound **2** (9.7 mg, 6.3%) according to its spectroscopic data.

3.7. Synthesis of PySCH$_2$(3,5-Me$_2$Pz) (Py = 2-pyridyl) (**9**)

To a stirred solution of EtONa (5.10 g, 75 mmol) in ethanol (75 ml) at 0 °C was added 2-mercaptopyridine (4.17 g, 37.5 mmol). The reaction mixture was continuously stirred for 30 min, and then 1-chloromethyl-3,5-dimethylpyrazole hydrochloride (6.34 g, 35 mmol) was added. Subsequently, the reaction mixture was stirred at ambient temperature for additional 3 h. The solvent was removed *in vacuo*, and water (75 ml) was added. The water phase was extracted with CH_2Cl_2 (3 × 50 ml). The organic layers were combined and dried over anhydrous $MgSO_4$. After removing the solvent, the residue was recrystallized from ethyl acetate/hexane to give yellow solids of **9** (3.37 g, 44%). ^{1}H NMR: δ 2.19, 2.26 (s, s, 3H, 3H, CH_3), 5.75 (s, 1H, H^4 of pyrazole), 5.85 (s, 2H, CH_2), 6.99–7.02,

7.19, 7.46–7.50, 8.45 (m, d, $J = 4.8$ Hz, m, d, $J = 8.0$ Hz, 1H, 1H, 1H, 1H, C_5H_4N) ppm. ^{13}C NMR: δ 11.2, 13.6 (CH_3), 47.6 (CH_2), 105.9 (C^4 of pyrazole), 120.3, 122.9, 136.5, 139.9, 148.8, 149.2, 156.4 (C_5H_4N, C^3 and C^5 of pyrazole) ppm. Anal. Calc. for $C_{11}H_{13}N_3S$: C, 60.24; H, 5.97; N, 19.16. Found: C, 60.10; H, 6.05; N, 19.30%.

3.8. Synthesis of $PySCH_2(3,5\text{-}Me_2Pz)Mo(CO)_4$ (**10**)

This complex was obtained by the reaction of $Mo(CO)_6$ and **9** as described above for complex **6**. The reaction time was 4 h. Yield: 46%. ^1H NMR: δ 2.32, 2.49 (s, s, 3H, 3H, CH_3), 5.88 (s, br, 3H, H^4 of pyrazole and CH_2), 7.15–7.19, 7.56–7.59, 7.70–7.75, 8.33–8.35 (m, m, m, m, 1H, 1H, 1H, 1H, C_5H_4N) ppm. ^{13}C NMR: δ 12.2, 16.1 (CH_3), 50.1 (CH_2), 107.3 (C^4 of pyrazole), 122.7, 124.2, 137.9, 142.2, 148.4, 148.5, 155.2 (C_5H_4N, C^3 and C^5 of pyrazole), 201.0, 205.5, 219.2, 220.3 (CO) ppm. IR: $\nu_{CO} = 2023.6$ (s), 1917.9 (vs), 1885.6 (vs), 1840.2 (vs) cm^{-1}. Anal. Calc. for $C_{15}H_{13}MoN_3O_4S$: C, 42.16; H, 3.07; N, 9.83. Found: C, 41.72; H, 3.42; N, 10.04%.

3.9. Synthesis of $PySCH_2(3,5\text{-}Me_2Pz)W(CO)_4$ (**11**)

This complex was obtained by the reaction of **9** and $W(CO)_5THF$ as described above for complex **7**. Complex **11** was purified by column chromatography on silica using CH_2Cl_2/hexane ($V{:}V = 2{:}1$) as eluent. Yield: 32%. ^1H NMR (acetone-d_6): δ 2.33, 2.59 (s, s, 3H, 3H, CH_3), 5.22 (d, $J = 13.0$ Hz, 1H, CH_2), 6.08 (s, 1H, H^4 of pyrazole), 6.66 (d, $J = 13.0$ Hz, 1H, CH_2), 7.35 (ddd, $J = 7.5$, 4.9, 1.0 Hz, 1H, C_5H_4N), 7.65 (dt, $J = 8.1$, 0.9 Hz, 1H, C_5H_4N), 7.96 (ddd, $J = 8.0$, 7.6, 1.8 Hz, 1H, C_5H_4N), 8.46 (ddd, $J = 4.9$, 1.8, 0.9 Hz, 1H, C_5H_4N) ppm. ^{13}C NMR (acetone-d_6): δ 11.7, 16.2 (CH_3), 51.4 (CH_2), 107.1 (C^4 of pyrazole), 123.4, 123.9, 138.5, 142.3, 149.1, 152.7, 155.0 (C_5H_4N, C^3 and C^5 of pyrazole), 201.1, 202.7, 210.1, 210.8 (CO) ppm. IR: $\nu_{CO} = 2017.0$ (vs), 1909.7 (vs), 1877.9 (vs), 1833.9 (vs) cm^{-1}. Anal. Calc. for $C_{15}H_{13}N_3O_4SW$: C, 34.97; H, 2.54; N, 8.16. Found: C, 34.92; H, 2.49; N, 8.38%.

3.10. Synthesis of $Ph_3SnCH(SPy)(3,5\text{-}Me_2Pz)$ (**12**)

This compound was similarly obtained as above-mentioned for compound **5**, while $PhSCH_2(3,5\text{-}Me_2Pz)$ was replaced by compound **9**. This compound was recrystallized from ethyl acetate to yield yellow crystals of **12**. Yield: 51%. ^1H NMR: δ 2.19, 2.29 (s, s, 3H, 3H, CH_3), 5.79 (s, 1H, H^4 of pyrazole), 5.97 (s, $^2J_{Sn-H} = 27.7$ Hz, 1H, CH), 6.86–6.90, 7.11, 7.41–7.44, 7.85 (m, d, $J = 8.0$ Hz, m, d, $J = 4.3$ Hz, 1H, 1H, 1H, 1H, C_5H_4N), 7.32–7.34, 7.57–7.76 (m, m, 9H, 6H, SnC_6H_5) ppm. ^{13}C NMR: δ 11.7, 13.3 (CH_3), 51.2 (CH), 107.1 (C^4 of pyrazole), 120.1, 122.9, 127.9, 128.1, 136.8, 136.9, 139.4, 143.8, 146.1, 147.9, 156.0 (C_5H_4N, SnC_6H_5 as well as C^3 and C^5 of pyrazole) ppm. Anal. Calc. for $C_{29}H_{27}N_3SSn$: C, 61.29; H, 4.79; N, 7.39. Found: C, 61.12; H, 4.87; N, 7.55%.

3.11. Synthesis of $PySCH(3,5\text{-}Me_2Pz)Mo(CO)_3SnPh_3$ (**13**)

This compound was similarly obtained as above-mentioned for compound **1** by the reaction of $Mo(CO)_6$ with compound **12**. The eluent was CH_2Cl_2/hexane ($V{:}V = 1{:}1$). Yield: 71%. ^1H NMR: δ 1.94, 2.27 (s, s, 3H, 3H, CH_3), 4.18 (s, 1H, CH), 5.76 (s, 1H, H^4 of pyrazole), 7.00–7.04, 7.23–7.26, 7.28–7.34, 9.24 (m, m, m, d, $J = 5.1$ Hz, 1H, 1H, 1H, 1H, C_5H_4N), 7.28–7.34, 7.49–7.66 (m, m, 9H, 6H, SnC_6H_5) ppm. ^{13}C NMR: δ 9.5, 12.2 (CH_3), 49.1 (CH), 104.7 (C^4 of pyrazole), 119.7, 122.5, 128.1, 128.3, 136.9, 137.1, 141.3, 143.9, 147.8, 153.3, 170.0 (C_5H_4N, SnC_6H_5 as well as C^3 and C^5 of pyrazole) ppm. No signal of carbonyl carbons was observed possibly due to the low signal intensity and the limited solubility of **13**. IR: ν_{CO} = 1974.4 (vs), 1888.9 (vs), 1859.4 (vs) cm^{-1}. Anal. Calc. for $C_{32}H_{27}MoN_3O_3SSn$: C, 51.36; H, 3.64; N, 5.62. Found: C, 51.86; H, 3.85; N, 5.57%.

3.12. Reaction of **13** with $P(OR)_3$ (R = Ph or Et)

The mixture of compound **13** (0.4 mmol) and $P(OR)_3$ (4 mmol) was stirred and heated at 80 °C for 4 h. After cooling to room temperature, the reaction mixture was washed with hexane to remove the excess of $P(OR)_3$, and the residue was purified by column chromatography on silica using CH_2Cl_2/hexane as eluent. The eluate was concentrated to dryness under a reduced pressure, and the residue was recrystallized from CH_2Cl_2/hexane or ethyl acetate/hexane to give red crystals.

Table 1
Crystal data and refinement parameters for compounds **2**, **4**, **5**, **7** and **10**.

Compound	**2**	**4**	**5**	**7**	**10**
Formula	$C_{16}H_{14}N_2O_4SW$	$C_{15}H_{14}Cl_4N_2O_3SSnW$	$C_{30}H_{28}N_2SSn$	$C_{34}H_{28}N_2O_4SSnW$	$C_{15}H_{13}MoN_3O_4S$
Formula weight	514.20	746.68	567.29	863.18	427.28
Crystal size (mm)	0.16 × 0.14 × 0.10	0.20 × 0.16 × 0.12	0.22 × 0.20 × 0.16	0.22 × 0.08 × 0.06	0.18 × 0.16 × 0.10
T (K)	294(2)	294(2)	294(2)	113(2)	113(2)
λ (Mo Kα) (Å)	0.71073	0.71073	0.71073	0.71070	0.71073
Crystal system	Monoclinic	Monoclinic	Monoclinic	Monoclinic	Triclinic
Space group	$P2_1/n$	$P2_1/c$	$P2_1/c$	$P2_1/c$	$P\bar{1}$
a (Å)	11.6448(19)	8.343(3)	15.623(3)	17.350(3)	8.4385(17)
b (Å)	13.695(2)	16.964(6)	10.1353(17)	9.7523(14)	8.4704(17)
c (Å)	11.6458(19)	16.455(5)	17.681(3)	19.370(3)	12.750(3)
α (°)	90	90	90	90	96.64(3)
β (°)	107.56(1)	98.278(6)	104.794(3)	100.517(2)	102.01(3)
γ (°)	90	90	90	90	105.78(3)
V (Å)^3	1770.5(5)	2304.8(13)	2706.7(8)	3222.5(8)	843.3(3)
Z	4	4	4	4	2
D_c (g cm^{-3})	1.929	2.152	1.392	1.779	1.683
F(000)	984	1400	1152	1672	428
μ (mm^{-1})	6.663	6.642	1.041	4.446	0.925
θ Range (°)	2.17–26.38	1.73–25.02	1.35–26.44	2.14–27.88	1.66–25.02
No. of unique reflections (R_{int})	3622 (0.0329)	4050 (0.0399)	5538 (0.0519)	7680 (0.0675)	2950 (0.0313)
No. of observed reflections ($I > 2\sigma(I)$)	2963	3276	3289	6739	2584
No. of parameters	218	246	309	391	219
GOF	1.042	1.083	1.003	1.037	1.118
Residuals R, Rw	0.0258, 0.0595	0.0267, 0.0533	0.0375, 0.0584	0.0305, 0.0689	0.0239, 0.0606

Table 2
Crystal data and refinement parameters for compounds **13** and **14**.

Compound	**13**.0.25CH_2Cl_2	**14**
Formula	$C_{32.25}H_{27.5}Cl_{0.5}MoN_3O_3SSn$	$C_{49}H_{42}MoN_3O_5PSSn$
Formula weight	769.49	1030.52
Crystal size (mm)	0.20 × 0.16 × 0.12	0.26 × 0.18 × 0.14
T (K)	113(2)	113(2)
λ (Mo Kα) (Å)	0.71073	0.71073
Crystal system	Monoclinic	Triclinic
Space group	$C2/c$	$P\bar{1}$
a (Å)	29.539(6)	9.3560(19)
b (Å)	15.229(3)	15.014(3)
c (Å)	18.250(4)	16.949(3)
α (°)	90	69.33(3)
β (°)	127.28(3)	89.63(3)
γ (°)	90	81.71(3)
V (Å)^3	6532(2)	2201.8(8)
Z	8	2
D_c (g cm^{-3})	1.565	1.554
F(000)	3060	1040
μ (mm^{-1})	1.289	0.987
θ Range (°)	1.74–25.02	4.79–26.00
No. of unique reflections (R_{int})	5751 (0.0393)	18607 (0.0428)
No. of observed reflections ($I > 2\sigma(I)$)	5114	18473
No. of parameters	416	555
GOF	1.113	1.176
Residuals R, Rw	0.0498, 0.1147	0.0839, 0.2126

3.12.1. Synthesis of $CH(NC_4H_4C{=}S)(3,5\text{-}Me_2Pz)Mo(CO)_2(P(OPh)_3)SnPh_3$ (**14**)

This compound was obtained by the reaction of **13** with P(OPh)$_3$. The reaction mixture was purified by column chromatography using CH_2Cl_2/hexane (V:V = 1:2) as eluent. Crystallization from CH_2Cl_2/hexane afforded red crystals of **14**. Yield: 39%. ^{1}H NMR: δ 1.60, 2.23 (s, s, 3H, 3H, CH_3), 5.28 (d, $^3J_{PH}$ = 2.8 Hz, 1H, CH), 5.65 (s, 1H, H^4 of pyrazole), 6.19, 6.84 (t, J = 6.6 Hz, d, J = 6.5 Hz, 1H, 1H, C_5H_4NS), 6.83–7.17, 7.35–7.46 (m, m, 24H, 8H, C_5H_4NS, SnC_6H_5 and OC_6H_5) ppm. ^{13}C NMR: δ 9.8, 12.6 (CH_3), 83.1 (d, J_{PC} = 48.9 Hz, CH), 106.3 (C^4 of pyrazole), 114.5, 121.4, 121.5, 124.2, 127.6, 127.8, 129.3, 132.3, 134.6, 136.9, 141.4, 144.9, 149.1 (C_5H_4N, SnC_6H_5, OC_6H_5 as well as C^3 and C^5 of pyrazole), 151.9 (d, J_{PC} = 11.6 Hz, OC_6H_5), 177.8 (d, J_{PC} = 10.5 Hz, C=S), 228.9 (d, J_{PC} = 32.9 Hz, CO), 229.8 (d, J_{PC} = 29.3 Hz, CO) ppm. ^{31}P NMR: δ 157.4 ppm. IR: ν_{CO} = 1896.0 (vs), 1824.7 (vs) cm^{-1}. Anal. Calc. for $C_{49}H_{42}MoN_3O_5PSSn$: C, 57.11; H, 4.11; N, 4.08. Found: C, 56.78; H, 4.37; N, 4.41%.

3.12.2. Synthesis of $CH(NC_4H_4C{=}S)(3,5\text{-}Me_2Pz)Mo(CO)_2(P(OEt)_3)SnPh_3$ (**15**)

This compound was obtained by the reaction of **13** with P(OEt)$_3$. The reaction mixture was purified by column chromatography using CH_2Cl_2/hexane (V:V = 1:1) as eluent. Crystallization from ethyl acetate/hexane afforded red crystals of **15**. Yield: 45%. ^{1}H NMR: δ 1.20 (t, J = 7.0 Hz, 9H, CH_2CH_3), 1.62, 2.29 (s, s, 3H, 3H, CH_3), 3.91 (q, J = 7.0 Hz, 6H, CH_2CH_3), 5.30 (d, $^3J_{PH}$ = 3.6 Hz, 1H, CH), 5.67 (s, 1H, H^4 of pyrazole), 6.28, 6.96, 7.08–7.20, 7.59 (t, J = 6.4 Hz, d, J = 6.4 Hz, m, d, J = 8.4 Hz, 1H, 1H, 1H, 1H, C_5H_4NS), 7.08–7.20, 7.41–7.53 (m, m, 9H, 6H, C_6H_5) ppm. ^{13}C NMR: δ 9.8, 12.5 (CH_3), 16.1 (d, J_{PC} = 6.3 Hz, CH_2CH_3), 60.7 (d, J_{PC} = 4.4 Hz, CH_2CH_3), 83.3 (d, J_{PC} = 46.8 Hz, CH), 106.1 (C^4 of pyrazole), 114.6, 127.6, 127.7, 132.3, 134.6, 136.9, 141.3, 141.6, 145.1, 149.1 (C_5H_4N, C_6H_5 as well as C^3 and C^5 of pyrazole), 177.8 (d, J_{PC} = 11.4 Hz, C=S), 231.0 (d, J_{PC} = 28.8 Hz, CO), 232.7 (d, J_{PC} = 32.5 Hz, CO) ppm. ^{31}P NMR: δ 171.0 ppm. IR: ν_{CO} = 1883.4 (vs), 1807.6 (vs) cm^{-1}. Anal. Calc. for $C_{37}H_{42}MoN_3O_5PSSn\cdot 0.5CH_3CO_2C_2H_5$: C, 50.34; H, 4.98; N, 4.52. Found: C, 49.98; H, 5.40; N, 5.00%.

3.13. Crystal structure determinations

Crystals of **2**, **4**, **7**, **10**, **13** and **14** suitable for X-ray analyses were obtained by slow diffusion of hexane into their CH_2Cl_2 solutions at −18 °C. While crystals of **5** suitable for X-ray analyses were obtained by slowly cooling its hot hexane solution. Intensity data were collected on a Bruker SMART CCD diffractometer for **2**, **4** and **5** as well as Rigaku Saturn CCD detector for **7**, **10**, **13** and **14**, respectively. Semi-empirical absorption corrections were applied using the SADABS program [20] for **2**, **4** and **5** as well as using the Crystalclear program [21] for **7**, **10**, **13** and **14**. The crystal of **14** was twinned and the reflection data were measured for the two twin domains, scaled and combined together using Twin solve in the Crystalclear program [21]. Overlapping reflections could not be satisfactorily measured and were discarded, leading to a data completeness of 90.2%. The structures were solved by direct methods and difference Fourier map using SHELXS of the SHELXTL package and refined with SHELXL [22] by full-matrix least-squares on F^2. All non-hydrogen atoms were refined anisotropically. A summary of the fundamental crystal data for **2**, **4**, **5**, **7**, **10**, **13** and **14** is listed in Tables 1 and 2, respectively.

Acknowledgements

This work is supported by the National Natural Science Foundation of China (Nos. 20672059 and 20721062).

Appendix A. Supplementary material

CCDC numbers 773775–773781 for **2**, **4**, **5**, **7**, **10**, **13** and **14** contain the supplementary crystallographic data for this paper. These data can be obtained free of charge from The Cambridge Crystallographic Data Centre via www.ccdc.cam.ac.uk/data_request/cif.

References

[1] A. Otero, J. Fernández-Baeza, A. Lara-Sánchez, J. Tejeda, L.F. Sánchez-Barba, Eur. J. Inorg. Chem. (2008) 5309–5326.
[2] C. Pettinari, R. Pettinari, Coord. Chem. Rev. 249 (2005) 663–691.
[3] A. Otero, J. Fernández-Baeza, A. Antiñolo, J. Tejeda, A. Lara-Sánchez, Dalton Trans. (2004) 1499–1510.
[4] Z.-K. Wen, Y.-F. Xie, S.-B. Zhao, R.-Y. Tan, L.-F. Tang, J. Organomet. Chem. 693 (2008) 1359–1366.
[5] L.-F. Tang, S.-B. Zhao, W.-L. Jia, Z. Yang, D.-T. Song, J.-T. Wang, Organometallics 22 (2003) 3290–3298.
[6] Z.-K. Wen, Z. Yang, H.-B. Song, L.-F. Tang, Chin. J. Chem. 27 (2009) 993–998.
[7] X.-Y. Zhang, J. Hong, H.-B. Song, L.-F. Tang, Organometallics 26 (2007) 4038–4041.
[8] L.-F. Tang, J. Hong, Z.-K. Wen, Organometallics 24 (2005) 4451–4453.
[9] A.R. Katritzky, J.N. Lam, Can. J. Chem. 67 (1989) 1144–1147.
[10] L.E. Orgel, Inorg. Chem. 1 (1962) 25–29.
[11] L.-F. Tang, W.-L. Jia, Z.-H. Wang, J.-T. Wang, H.-G. Wang, J. Organomet. Chem. 649 (2002) 152–160.
[12] L.-F. Tang, W.-L. Jia, X.-M. Zhao, P. Yang, J.-T. Wang, J. Organomet. Chem. 658 (2002) 198–203.
[13] W. Levason, L.P. Ollivere, G. Reid, N. Tsoureas, M. Webster, J. Organomet. Chem. 694 (2009) 2299–2308.
[14] V.C. Gibson, N.J. Long, R.J. Long, A.J.P. White, C.K. Williams, D.J. Williams, E. Grigiotti, P. Zanello, Organometallics 23 (2004) 957–967.
[15] N.L. Allinger, X. Zhou, J. Bergsma, J. Mol. Struct. (THEOCHEM) 312 (1994) 69–83.
[16] D.C. Ghosh, T. Chakraborty, B. Mandal, Theor. Chem. Acc. 124 (2009) 295–301.
[17] Y.-F. Xie, Z.-K. Wen, R.-Y. Tan, J. Hong, S.-B. Zhao, L.-F. Tang, Organometallics 27 (2008) 5684–5690.
[18] R.M. Silva, M.D. Smith, J.R. Gardinier, J. Org. Chem. 70 (2005) 8755–8763.
[19] C. Gwengo, R.M. Silva, M.D. Smith, S.V. Lindeman, J.R. Gardinier, Inorg. Chim. Acta 362 (2009) 4127–4136.
[20] G.M. Sheldrick, SADABS, Program for Empirical Absorption Correction of Area Detector Data. University of Göttingen, Germany, 1996.
[21] Crystal Structure 3.7.0 and Crystalclear 1.36: Crystal Structure Analysis Package. Rigaku and Rigaku/MSC, TX, 2000–2005.
[22] G.M. Sheldrick, SHELXS97 and SHELXL97. University of Göttingen, Germany, 1997.